International Journal of Heat and Fluid Flow 74 (2018) 144–153

Contents lists available at ScienceDirect

International Journal of Heat and Fluid Flow

journal homepage: www.elsevier.com/locate/ijhff

Coherent structures in turbulent square duct flow

Rastin Matin[*,a], Leo H.O. Hellström[*,b], Anier Hernández-García[a], Joachim Mathiesen[a], Alexander J. Smits[b]

[a] Niels Bohr Institute, University of Copenhagen, Copenhagen, DK-2100, Denmark
[b] Mechanical and Aerospace Engineering, Princeton University, Princeton, NJ 08544, United States

ARTICLE INFO

Keywords:
Square duct
Turbulent flow
CFD
POD
Coherent structures

ABSTRACT

The current work investigates coherent structures in a direct numerical simulation of turbulent flow in a square duct at a Reynolds number of 3800. The flow is investigated using proper orthogonal decomposition (POD). The higher order POD modes reveal corner structures spanning a wide range of scales, supporting the hypothesis that the secondary motions are composed of a superposition of contributions from instantaneous organized motions of different scales. The lower order POD modes are identified as representing the turbulence coherent structures. The streamwise evolution of the structures is investigated using conditional modes, which resolve structures similar to the large-scale motions found in other wall-bounded turbulent flows. These large-scale structures have a streamwise length $O(5-8h)$, similar to what has been observed experimentally and numerically in circular pipe flow. The evolution is characterized by a wall-normal growth followed by a wall-detachment, after which the transition to a new structure occurs. It appears that there is a transition between a symmetric and anti-symmetric mode, resulting in in-phase and out-of-phase motions at the opposing walls.

1. Introduction

Turbulent flow in a square duct is distinguished by the formation of corner vortices due to spanwise gradients of the Reynolds stress. This phenomenon is commonly referred to as a secondary flow of Prandtl's second kind, and they only occur above a threshold Reynolds number. They are absent in laminar flows, and stand in contrast to secondary flows of the first kind that appear in ducts or pipes with streamwise curvature, which can be found in both laminar and in turbulent flows. The flow in fully turbulent square duct exhibits four statistically symmetric quadrants, each with a pair of counter rotating vortices, as illustrated in Figs. 1(a, b). Each vortex pair moves high momentum fluid along the corner bisector (the diagonals of the duct) from the core region towards the corner with a characteristic velocity that is about 1–3% of the bulk velocity U_B. At the same time, the interaction between neighboring vortex pairs (situated in neighboring corners) moves low momentum fluid away from the midpoint of each wall towards the core region, along the (y, z) coordinate axes in Fig. 1(a) (Gavrilakis, 1992; Ham et al., 2000; Humphrey et al., 1981; Madabhushi and Vanka, 1991). However, Uhlmann et al. (2007) found that a marginally turbulent duct flow was governed by two meta-stable regimes where the quadrant symmetry was broken. These asymmetric states were found to have a characteristic lifetime of order $O(10^3 h/U_B)$, where h is the duct half-height. The first of these states is shown in Figs. 1(c, d), where the two counter rotating vorticies along the top and bottom wall are more prominent than those along the side walls. The second state is similar to the first, while subject to a 90° degree rotation. Uhlmann et al. (2007) further concluded that they needed a sample length of $1639h/U_B$ in order to attain a fully symmetric mean flow (one that was symmetric with respect to both coordinate axes and duct diagonals).

The secondary motions are also important in changing the turbulence statistics. Huser and Biringen (1992), for example, performed a direct numerical simulation (DNS) at a bulk Reynolds number $Re_B = U_B 2h/\nu = 10\,000$ (ν is the kinematic viscosity), and showed that the streamwise component of the Reynolds stress ($\overline{u^2}$) takes its peak value $0.05h$ from the wall, at a spanwise distance of $0.6h$ from the corner, coinciding with the location of the center of the corner vortex. They also found a similar relationship for the Reynolds shear stress ($-\overline{uv}$). However, Humphrey et al. (1981) performed an experiment at $Re_B = 40\,000$, and showed instead that the peak location for ($\overline{u^2}$) was at a spanwise distance of $1h$ from the corner (that is, in the plane of symmetry), raising the possibility that the effects of the secondary flows on the turbulence depend on Reynolds number.

In this respect, Brundrett and Baines (1964) demonstrated that for $20\,000 \leq Re_B \leq 83\,000$ the basic pattern of the secondary motions is independent of the Reynolds number if scaled with U_B. They found,

* Corresponding authors.
E-mail addresses: rastin@nbi.ku.dk (R. Matin), lhellstr@Princeton.edu (L.H.O. Hellström).

https://doi.org/10.1016/j.ijheatfluidflow.2018.08.007
Received 18 March 2018; Received in revised form 27 June 2018; Accepted 24 August 2018
0142-727X/ © 2018 Elsevier Inc. All rights reserved.

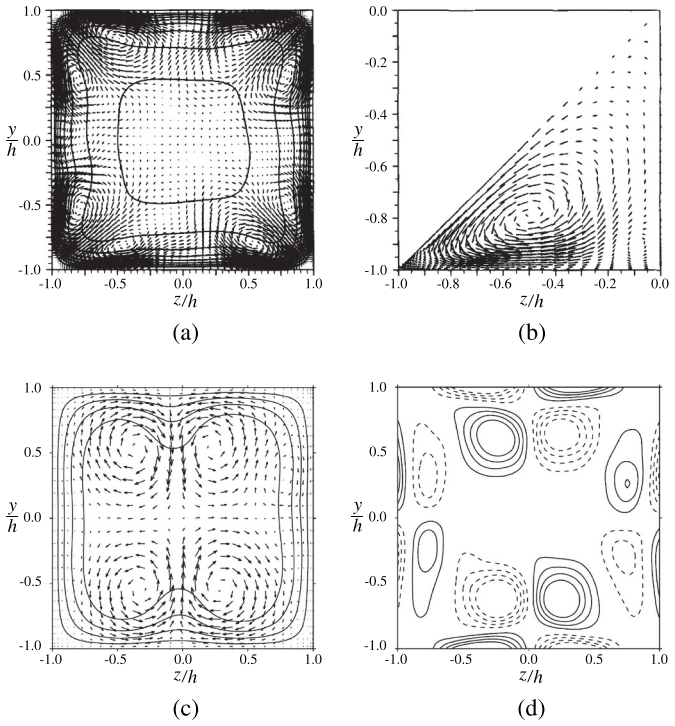

Fig. 1. (a) Secondary flow of Prandtl's second kind in turbulent flow through a square duct, computed at $Re_B = 4410$. Vectors represents the in-plane motions while contours represents streamwise velocity with increments of $4u_\tau$ and (b) zoomed-in view of the third quadrant of (a). Figures adapted from Gavrilakis (1992). Note that Uhlmann et al. (2007) showed that the quadrant symmetry may be broken for a marginally turbulent flow; (c) shows contour lines representing mean axial flow at $Re_B = 2410$, and vectors show the in-plane components; (d) displays isocontours of average streamwise vorticity, computed at $Re_B = 2286$. Figures (c) and dummy TXdummy- (d) are adapted from Uhlmann et al. (2007).

however, that although the location of the corner vortices were unchanged, they penetrated further into the corner as the Reynolds number increased. Pinelli et al. (2010) conducted DNS for $2154 \leq Re_B \leq 7000$ and found that the cores of the mean vortical structures initially approach the corner as the Reynolds number increases, and then reach a fixed location scaled with h for $Re_B \geq 4410$. They proposed that the collapse in outer coordinates (that is, with h) provides a possible link between the secondary motions and the coherent motions of wall-bounded turbulence, in particular the large-scale motions (LSMs). They further noted that the pattern of the secondary motion stretches along the corner bisector away from the corner as the Reynolds number increases, and they suggested that this phenomenon was due to a superposition of contributions from instantaneous organized motions at different scales.

Broadly speaking, the organized motions in turbulent wall-bounded flows can be classified into four distinct groups (Smits et al., 2011). Ordered by their size, the first group is identified as the near-wall streaks located in the viscous sublayer with a typical spanwise spacing of $100\nu/u_\tau$, where u_τ is the friction velocity ($= \sqrt{\tau_w/\rho}$, where τ_w is the shear stress at the wall and ρ is the fluid density). The second category is the hairpin-vortex, which spans a wide range of scales with a lower height limit of about $100\nu/u_\tau$. The hairpin-vortices are believed to align into packets convecting at a common velocity, creating the third group often referred to as the large-scale motions (LSMs) with a streamwise length scale of $O(2-3\delta)$ (Adrian et al., 2000). The last group is known as superstructures in boundary layer flows and very-large-scale motions (VLSMs) in pipe flow. They are characterized by a long meandering region of low momentum fluid with a streamwise extent $O(7\delta)$, but may occasionally extend as far as 30δ, where δ represents the outer length scale (Kim and Adrian, 1999; Monty et al., 2007). The origin of the VLSMs is still undetermined but is believed to be due to a pseudo-streamwise alignment of LSMs (Kim and Adrian, 1999; Hellström et al., 2015), while the cause of the alignment is unknown.

The identification of organized motions in turbulent wall-bounded flows has been approached using flow visualizations, spatial and temporal correlations, and by identifying regions of uniform-momentum (Adrian et al., 2000; Bailey et al., 2008; Dennis and Sogaro, 2014; Morris et al., 2007; Wu and Moin, 2008). It has been shown that proper orthogonal decomposition (POD), a two-point correlation approach, is well suited to decompose the flow structures into a set of energetic motions (Moin and Moser, 1989; Duggleby et al., 2007; Hellström et al., 2011; Baltzer et al., 2013; Hellström et al., 2015). Hellström et al. (2016a) used POD to investigate the structures in a transitional pipe flow at $Re_D = U_B 2R/\nu = 3440$, which were compared to the fully turbulent cases at $Re_D = 51\,700$ and $104\,000$ reported by Hellström et al. (2015). It was shown that over this entire Reynolds number range the large-scale structures were remarkably similar and shared many features with the LSM. The evolution between consecutive structures was characterized by the detachment and decay of an existing structure and the initiation of a new structure at the wall. The majority of this work has been performed on either axisymmetric pipe flow or channel flow, while little is known of the organized motions in a square duct. To understand this aspect of duct flow better, we performed a direct numerical simulation of flow in a square duct at $Re_B = 3800$. We apply a POD analysis to identify the mean flow features along with the corner vortices and we use a conditional-average approach to visualize the dynamics of the coherent structures, based on the procedures developed by Hellström et al. (2015).

2. Computational details

2.1. Lattice Boltzmann method

We perform a direct numerical simulation of an incompressible turbulent flow through a square duct at Reynolds number $Re_B = 3800$. The simulations were performed using the lattice Boltzmann method, where fictive particles are successively advected and collided. The particle dynamics can be shown analytically to yield a hydrodynamic behavior consistent with the incompressible Navier-Stokes equations (see, *e.g.*, Benzi et al. (1992)), given by

$$\partial_t \rho + \nabla\cdot(\rho\mathbf{u}) = 0 \tag{1}$$

$$\partial_t \mathbf{u} + (\mathbf{u}\cdot\nabla)\mathbf{u} = \mathbf{f} + \nabla\cdot\nu(\nabla\mathbf{u} + (\nabla\mathbf{u})^T). \tag{2}$$

The fluid is initially at rest and driven to a steady state by an external constant body force **f** acting in the streamwise direction. Because lattice Boltzmann schemes generally suffer from compressibility effects of $O(Ma^2)$, where Ma is the Mach number, the simulation parameters are therefore chosen such that $Ma < 0.01$. Further details regarding the numerical scheme and its implementation may be found in Misztal et al. (2015); Matin et al. (2017).

2.2. Grid considerations

The global domain measures $(x, y, z) = \{80h, 2h, 2h\}$, and the simulation is based on an unstructured grid with a periodic boundary condition in the streamwise direction. Since the lower bound on the dissipation length scale is approximately twice the viscous length scale (Yakhot et al., 2010), the grid spacing was chosen so that $[\Delta_x^+, \Delta_y^+, \Delta_z^+] \lessapprox [2, 2, 2]$, where $\Delta^+ = \Delta u_\tau/\nu$. The resulting mesh at the duct wall consists of 80 elements in the spanwise and 3200 elements in the streamwise directions. The resolution of the unstructured mesh is slightly denser within the domain itself, resulting in a total of 27×10^6 tetrahedral elements. A cross-section of the unstructured grid is shown in Fig. 2. We will label the wall at $y/h = 1.0$ as the upper wall, the one

Download English Version:

https://daneshyari.com/en/article/11023701

Download Persian Version:

https://daneshyari.com/article/11023701

Daneshyari.com